Semnan University

Journal of Modeling & Simulation in Electrical & Electronics Engineering (MSEEE)

Journal homepage: **https://mseee.semnan.ac.ir/**

ISSN: 2821-0786

Coordinated Fuzzy Control of SSSC and SMES for Frequency Control in a DFIG Integrated Power System

Ahmad Sasani[1], Mostafa Sedighi-zadeh[2] and Reza Keypour [•3]

***Abstract*--Nowadays, one of the features of developed countries is that they benefit from a highly reliable and stable electricity grid. In recent decades, the growth of power electronics technology has assisted this development. Flexible alternating current system (FACTS) devices are power electronics devices in the AC transmission grid. This paper evaluates the static synchronous series compensator (SSSC) in series with the transmission line and superconducting magnetic energy storage (SMES) placed at the end of the line to reduce grid frequency disturbances. The challenge is addressed by finding the optimal values for SSSC and SMES in the transmission grid using fuzzy logic, which is based on human decisions. Moreover, this paper investigates the effect of the presence and absence of variable-speed doubly-fed induction generator (DFIG)-type wind turbines. By increasing the penetration of variable-speed wind turbines in the grid, the equivalent system inertial is reduced, the ability to adjust the grid frequency is weakened, and the possibility of instability and even grid collapse after the frequency drop is increased. To this end, upon detection of frequency deviation in the grid, additional power is applied to the power system as a function of the grid frequency deviation by allocating a wind turbine with a control loop. In the absence of DFIG, the effect of only the optimized SMES-SSSC is investigated. This simulation is conducted using MATLAB/Simulink, and it is indicated that the error signal in determining the SMES and SSSC parameters is significantly reduced compared to previous studies, thanks to employing the fuzzy algorithm.**

***Index Terms*-- Optimum point, DFIG, Fuzzy, SSSC, SMES.**

I. INTRODUCTION

ONE of the main criteria for measuring the stability of a power system is maintaining a balance between energy production and consumption [1]. The balance is disturbed for a short interval, and the power frequency encounters deviations when a large power plant is disconnected or a large load is connected to the system. According to [2], [3], the frequency control loop is not suitable for solving this issue due to its slow performance in this system. One of the solutions was SMES, which suitably deals with frequency stability. In [4], in addition to the above issue, the load imposed on the transmission grid has increased in recent years. This increase will continue due to the increase in the number of single generators separate from the electricity companies, as well as the increase in competition between the companies themselves. Moreover, obtaining new boundaries for transmission lines has become very difficult. Increased load and lack of long-term design have led to the emergence of FACTS technology.

Various studies [5]-[7] have investigated various models to analyze the connection of two-zone systems. These studies have considered the role of SMES in each zone and the use of FACTS equipment to reduce frequency disturbances.

In previous studies, combinations such as SMES-SMES,

Received; 2024-10-13 Revised; 2025-04-08 Accepted; 2025-09-24

[1] Faculty of Electrical and Computer Engineering, Semnan University, Semnan, Iran.
[2] Faculty of Electrical and Computer Engineering, Shahid Beheshti, Tehran, Iran.
• Corresponding author Email: rkeypour@semnan.ac.ir

Cite this article as:
Sasani, A., Sedighi-zadeh, M. and Keypour, R. (2025). Coordinated Fuzzy Control of SSSC and SMES for Frequency Control in a DFIG Integrated Power System. *Journal of Modeling & Simulation in Electrical & Electronics Engineering (MSEEE).* Semnan University Press . *5 (2),* 1-9.
DOI: https://doi.org/10.22075/mseee.2025.34911.1182

SSSC-SMES, and Thyristor-Controlled PhaseShifter-superconducting magnetic energy storage(TCPS-SMES) have been compared with existing control structures and governors, and their performance against load and frequency disturbances has been investigated. The results have shown an improvement in system stability; however, factors such as the increase in equipment cost in each area, the difference between simulated models and real conditions, and the lack of a competitive market in some studies have caused the results to deviate from practical conditions.

In [8], frequency oscillation reduction has been investigated using one SMES in each region and employing combinations such as SSSC-SMES and TCPS-SMES to connect the two regions. However, achieving the desired frequency in this method requires high costs for installing SMES and FACTS equipment in each region.

In [7]-[8], other studies have investigated different optimization algorithms, such as CRPSO-PSO-GA-Tabu Search, to determine the parameters of SMES and FACTS devices based on the error signal. The results of the Cooperative Random Particle Swarm Optimization (CRPSO) algorithm show the best performance among these algorithms.

In [9], DFIG systems with control circuits introduced at the junction of two regions without using FACTS and SMES devices were investigated, and it was shown that these systems reduce the error signal. However, the said reduction comes at a higher cost than the changes caused by FACTS and SMES devices.

According to [10]-[11], SSSC is a voltage source converter (VSC) that, compared to series variable impedance compensators, provides power flow control in a way that variable impedance compensators cannot. Unlike impedance compensators, SSSC provides reactive power and requires isolation at lower voltages because it is indirectly connected to the transmission line through a coupling transformer. SSSC combined with SMES reduces power fluctuations and better coordinates oscillating machines. The evaluation of coordination between SSSC and SMES with DFIGs [12] and without DFIGs [13] has only been done in the context of a competitive market.

In [14], frequency deviations caused by load changes are reduced by introducing a two-area configuration, considering competitive market conditions, and using SMES storage element in one area and a FACTS device (TCPS) in the interconnection point with a DFIG.

Based on the review of the sources, SSSC has been chosen as the primary option due to its simultaneous control of active and reactive power, effective performance under varying load and network conditions, cost and system complexity reduction, and improved dynamic stability. These advantages make SSSC preferable over other compensators, including STATCOM, in this study.

Nonetheless, in all these cases, the equipment installed in the system must be replaced by other equipment, noting that changing a series of equipment will often be costly and impose great damage from a practical viewpoint. The presence of some equipment in each area, although it reduces the error signal, increases the cost of installing new equipment and removing the devices used in the current system, while complicating the equations governing the system. In that case, the probability of failure will increase. The presence of DFIGs at some points may not be possible for frequency stability. Therefore, using the fuzzy algorithm for optimizing SSSC and SMES parameters shows that a two-area connection, considering the competitive market conditions with and without DFIGs, can significantly reduce the frequency disturbances caused by load changes. This has not been achieved in the literature.

In this study, using fuzzy optimization, we seek:

- Determining the optimal values of the linearized SMES,
- Determining the optimal values of the linearized SSSE,
- Reducing the error signal due to the connection of two thermal-thermal and hydro-hydro areas, and
- Reducing distortion at each frequency output from two thermal-thermal and hydro-hydro areas

This article is organized as follows. Section 2 includes the introduction of the model under study, which describes the connection of two thermal-thermal and hydro-hydro power plants and the location of SMES, SSSC, and DFIG. This section presents the linearized models of SSSC, SMES, and DFIG, along with the inertia control loop related to DFIG. Section 3 includes fuzzy optimization and how to apply it to this study. Section 4 presents the output of simulation models in MATLAB software, and Section 5 provides the analysis and review of simulation results.

II. Case Study model

Although power system models are generally nonlinear, a linear model is considered for load-frequency control system studies. Fig. 1 shows a diagram of a two-area power system, neglecting all its electrical dynamics and only considering slow system dynamics, including governor and turbine speed. In this section, a two-area system is considered as a power system that includes a thermal power plant and a hydroelectric power plant. This model consists of four main parts:

- Distribution company (DISCO) model
- Generation company (GENCO) model
- Models of FACT devices
- Wind turbine

Fig. 1 presents a general multi-area frequency load control model suitable for competitive markets. In today's power systems, control areas may consist of different sources such as hydro, thermal, gas, or renewable units. Frequency load control studies have been performed on conventional power systems, which include hydro and thermal units. However, these studies have not been performed on systems with a restructured environment.

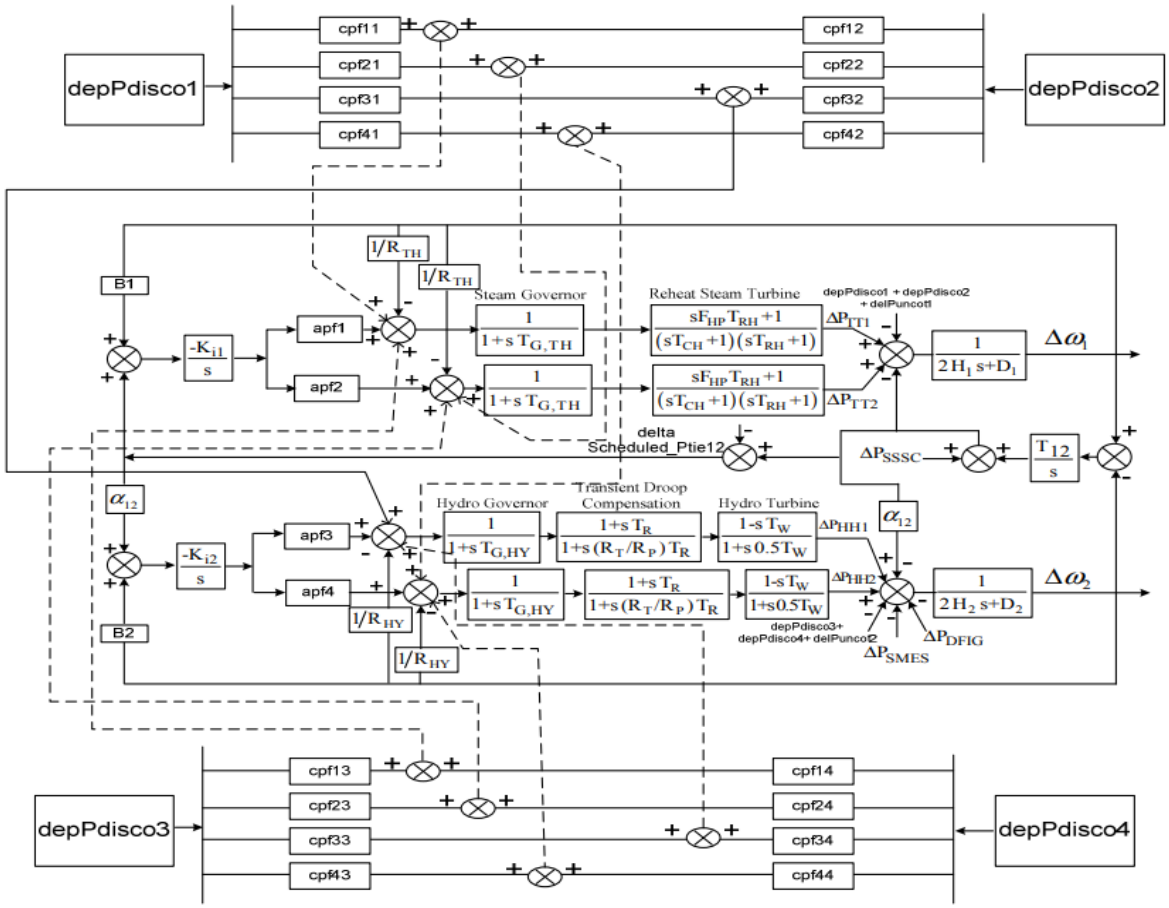

Fig. 1. Case study model including two thermal-thermal and hydro-hydro areas [12]

A. GENCO and DISCO Models

The load frequency control (LFC) in a restructured market must be designed to comply with all possible trades, such as intra-area trades, free contract trades, and other contracts. Several instances of these transactions may occur simultaneously in competitive electricity markets. A DISCO in each control area can engage with GENCOs in the same control area or other areas with bilateral contracts. GENCOs in such contracts change their output power to supply the contract load as long as it does not exceed the contract value. DISCO is responsible for maintaining market demand regulation following the contract agreement. The participation matrix of DPM units is used to execute transactions. The number of rows and columns in DPM represents the number of GENCOs and DISCOs, respectively. Each array of the DPM matrix is defined as a contract participation factor. Spfk1 is the contractual participation factor between the *k*th GENCO of the first DISCO. Spfk1 corresponds to the fraction of the total load power that 1-DISCO receives from GENCO-K on a contract basis. It is worth noting that $\sum_K cpf_{k1} = 1$. DPM indicates the participation of a DISCO in a contract with a GENCO. According to Fig. 1, each control area in this study has two generation units and two distribution units. It is assumed that a certain set of GENCOs must follow the total load required by the DISCOs [13,17].

As a result, the information signals must go from DISCO to a specific GENCO and specify the corresponding demands. In addition, unforeseen loads may be present in the control areas.

The DPM matrix that provides the participation factor of each unit will be as follows:

$$DPM = \begin{bmatrix} cpf_{11} & cpf_{12} & cpf_{13} & cpf_{14} \\ cpf_{21} & cpf_{22} & cpf_{23} & cpf_{24} \\ cpf_{31} & cpf_{32} & cpf_{33} & cpf_{34} \\ cpf_{41} & cpf_{42} & cpf_{43} & cpf_{44} \end{bmatrix}$$

The planned power of the tie line in the steady-state is obtained as (1):

$$\Delta P_{tie12.\text{sch}} = \left(P_{exp1}\right) - \left(P_{imp1}\right) \quad (1)$$

That the total power output from control area 1 (P_{exp1}) is equal to the demand of DISCOs in control area 2 from GENCOs of control area 1, and the total power input to control area 1 (P_{imp1}) is equal to the demand of DISCOs in control area 1 from GENCOs in control area 2.
In general, we have:

$$\Delta P_{tie12} = (\Delta P_{SSSC}) \left(\frac{T_{12}}{S}\right) (-\Delta F_2) \quad (2)$$

The error in the tie-line power ($\Delta P_{tie12error}$) is defined as (3):

$$\Delta P_{tie12.error} = (\Delta P_{tie12}) - \left(\Delta P_{tie12,sch}\right) \Delta P_{tie12.error} \quad (3)$$

In steady-state, it tends to zero when the actual tie-line power flow ($\Delta P_{tie12,error}$) reaches the planned power flow of the line. The control error of each area can be expressed as follows:

$$ACE_1 = B_1 \Delta f_1 + \Delta P_{tie12,error} \quad (4)$$

$$ACE_2 = B_2 \Delta f_2 + \alpha_{12} \Delta P_{tie12,error} \quad (5)$$

where, ACE_1 and ACE_2 are control areas 1 and 2, respectively. B_1 and B_2 are the frequency bias constants of areas 1 and 2, respectively, and α_{12} denotes the capacity of the control area.

B. Static Synchronous Series Compensator (SSSC)

The static Synchronous Series Compensator (SSSC) is a synchronous VSC placed in series with the transmission system. The real power required by the SSSC to exchange with the power grid is provided by a DC power source (battery or capacitor located on the DC side of the converter). The output voltage in SSSC is by controlling the conductance time of the switches in the VSC. Therefore, under any circumstances (steady/transient), the power of the transmission line is controlled by adjusting the SSSC output voltage.

The main applications of SSSC are dynamic control of power flow, dynamic control of voltage, and improving transient stability.

Fig. 2 illustrates the structure and configuration of the SSSC connected in series to a two-area grid.

Finally, the block diagram of the compensator is placed negatively in the feedback path as (6) [13]:

$$\Delta P_{sssc}(s) = K_1 \left(\frac{K_{sssc}}{1+T_{SSSC}}\right) \left(\frac{1+P_1 S}{1+P_2 S}\right) \left(\frac{1+P_3 S}{1+P_4 S}\right) \Delta\omega_m(s) \quad (6)$$

Where K_1, K_{SSSC}, T_{SSSC}, P_1, P_2, P_3, P_4 and $\Delta\omega_m$ represent stabilization gain, the SSSC gain, the time constant associated with SSSC, the phase compensation parameters, and frequency deviation, respectively.

C. SMES

SMES is used for energy storage, and its model is expressed as (7) [13]:

$$\Delta P_{smes}(s) = \left(\frac{K_{smes}}{1+ST_{SMES}}\right) \left(\frac{1+ST_1}{1+ST_2}\right) \left(\frac{1+ST_3}{1+ST_4}\right) \Delta\omega_m(s) \quad (7)$$

Where K_{smes}, T_{SMES}, T_1, T_2, T_3, and T_4 describe the gain and time constant of the SMES system, the time constant associated with SMES, respectively.

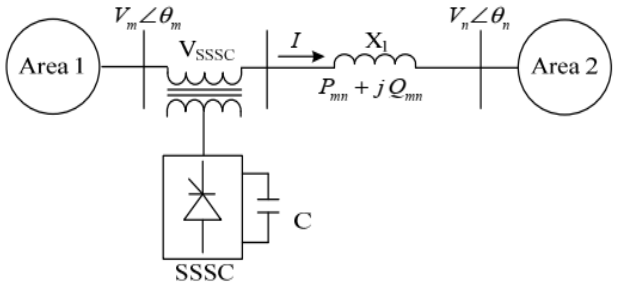

Fig. 2. Structure of SSSC in the two-area power system[13]

D. Wind turbine

With the expansion of wind energy use, the participation of wind turbines connected to doubly-fed induction generators (DFIGs) has increased. The activity of such generators in the conditions of variable winds has led to the improvement of their application. The widespread presence of this type of turbine reduces the participation of synchronous generators in the network, followed by increasing problems such as frequency control in the power system. With the advent of power electronics in this model of generators, the speed of rotation of this type of generator has been separated from the network, and changes in network frequency by the rotor of these generators are not considered. In general, the power plant is not involved in frequency control, and ultimately leads to the loss of stability of the network. According to several studies conducted by researchers on the problems of using wind turbines, such as the frequency deviation of the system, the performance of a fixed-speed induction generator by sharing its inertia is similar to that of a synchronous machine. However, it is not the case for DFIG. Thus, a control loop was considered to solve the problem. Thereby, variable-speed wind turbines have higher kinetic energy than fixed-speed turbines and can increase the active power during turbulence.

To regulate the network frequency, a signal called inertia control has been added to the power control loop of the variable-speed turbine. This loop operates during frequency deviation by increasing the amount of power stemming from the kinetic energy stored in the rotating part of the blades, seeking to improve the frequency dynamics of the power system in the initial moments after turbulence. To control this mode, one can adopt the proportionality of frequency derivative with additional power and/or control the initial frequency setting of the turbine or employ both strategies [16].

1) The Dynamic Model of Speed-Variable Wind Turbine

Fig. 3 presents the wind turbine model, incorporating detailed representations of its various components, each described using the relationships outlined in equations 8 to 13. Equation (8) illustrates the mechanical power, a function of the pitch angle, rotor speed, and wind speed [12].

$$P_m = \frac{\rho}{2} A_r V_w^3 C_p(\lambda.\theta) \quad (8)$$

In this equation, ρ is the density of air, VW is wind speed, and Cp is the power factor, which is a function of λ and θ. λ is the ratio of the tip speed of the rotor blade to the wind speed, and θ is the pitch angle of the blade. Cp is a characteristic of the wind turbine and is usually defined in terms of λ and θ.

The Cp curves for the GE wind turbine in terms of λ are plotted in Fig. 4. The Cp curve representation is as (9) [12]:

$$C_p(\lambda.\theta) = \sum_{i=0}^{4} \sum_{j=0}^{4} \alpha_{i.j} \theta^i \lambda^j \quad (9)$$

Curve fitting is a good approximation for the values 2 < λ < 13. Values of λ outside this range indicate very high and low wind speeds outside the turbine's operating range. According to the Cp curves of Fig. 4 in the variable-speed turbine, the speed is controlled according to the wind speed in a way specified for θ, the turbine operates at the peak point, and maximum power is generated.

For tracking purposes, the turbine's maximum reference speed is suitable for measured power, which is more accurate than measuring wind speed. The speed reference is 1.2 p.u. and is reduced for power levels below 75%, which is obtained according to E. (10) [12]:

$$w_{ref} = 0.67^2 + 1.42P + 0.51 \quad (10)$$

P is the measured power. The pitch step is used when the power levels exceed the nominal value.

2) Inertia Control Method

Using power electronics, the slip in the variable-speed turbine remains constant, and the rotor does not see changes in grid frequency, causing it to release its inertia first and eventually share its energy with the grid.

According to the above explanations, instability is created, which, according to the reference articles, an auxiliary signal is placed in the turbine so that during network frequency deviation, an excess power that is a function of the frequency deviation enters the network (refer to Fig. 5).

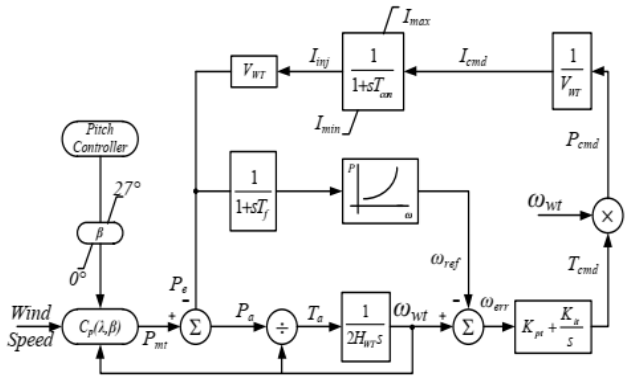

Fig. 3. Simplified model of a wind DFIG-type turbine along with real power and pitch angle controllers [12]

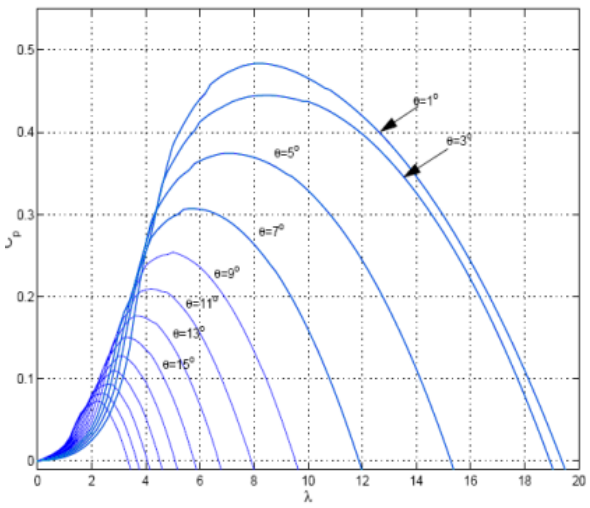

Fig. 4. C_p curves of wind power [12]

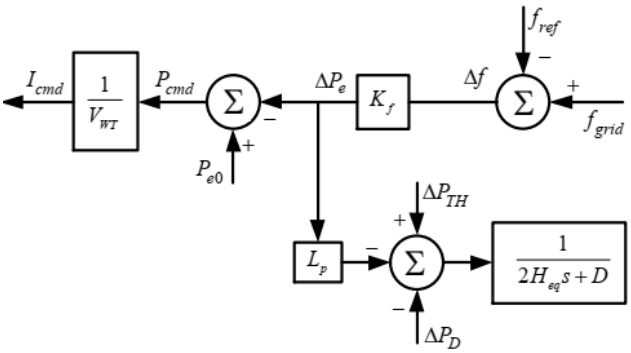

Fig. 5. The complementary control loop of the wind turbine [12]

The penetration level of wind turbines power to LP is shown in the figure. Thus, if LP is the percentage of generation, then LP can be considered the amount of system energy reduction in the absence of wind power. Kf is the coefficient of turbine participation in frequency control, improving the power system's frequency dynamics. However, it may reduce the turbine speed and cause it to deviate from the minimum speed. Therefore, Kf should be a number between frequency improvement and perturbation prevention.

The following equations include inertia equivalent to the network without the participation of the turbine (11) and the variable-speed wind turbine (12), in which frequency control with LP% of wind power participates, and the droop of generation units in both cases (13) [12].

$$H_{eq.lp} = H_{eq}(1 - L_p) \quad (11)$$

$$H_{eq.lp} = H_{eq}(1 - L_p) + H_{wt} L_p \quad (12)$$

$$R_{lp} = R/(1 - L_p) \quad (13)$$

III. Fuzzy Algorithm

The fuzzy theory was first introduced in 1965 by Zadeh. He pointed to the inability of classical mathematics to deal with inaccurate real-world problems, and established the

foundation of a new framework called fuzzy theory and introduced its foundations. The word *fuzzy* means vague.

Fuzzy theory is a new framework that can model reality as it is. The new fuzzy framework tries to bring the model closer to reality and reduce the gap between modeling and human thinking. This framework provides a suitable platform for defining fuzzy words, such as low, medium, and high, which agree with the human way of thinking and feeling [18,19].

A fuzzy set is determined through the membership function, the smooth and soft curve of which is more in line with human thinking and behavior. In contrast, in a classic set, the membership function is stepwise and binary, which cannot describe the true way of human thinking.

Constructing membership functions for fuzzy words related to a variable includes both the general form of the membership function and its parameters. There are several methods for determining membership functions, all of which are based on the subjective and experience of individuals, and in each field, are usually determined by experts in the field.

In this method, we will go through the following steps: first, the input numbers are fuzzified, then, using the implication of Zadeh and determining the type of statements with the help of MATLAB software, the type of combination and the desired output are obtained, and by placing it in SSSC and SMES blocks, the value of the FDM error signal is calculated.

IV. Model Description in Simulations

The linear model drawn in MATLAB/Simulink environment includes the connection of two power plants with the presence of DFIG. We evaluated it under six conditions. At the first three stages, with the basic values of the power plants without the presence of FACTS and DFIG devices, and the DFIG was added in the third stage, which improved the error signal. In the end, simulations were implemented in the presence of SSSC and SMES for the DFIG-type turbine.

A: Test Scenarios:

The following test scenarios are considered for the simulation. **Case 1***)* Two units of Thermal and Hydro are considered in area 1 and area 2, respectively, (TT-HH Model).

Case 2*)* 20% wind power penetration is considered in the area

Case 3) 20% wind power penetration is considered in area 2. The DFIG provides any short-term active power support (TT-HHW with f-Support Model)

Case 4) Extension of Case 1 with SSSC-SMES

Case 5) Extension of Case 2 with SSSC-SMES

Case 6) Extension of Case 2 with SSSC-SMES

Table I shows the optimized parameters for power plant input and FACTS devices. These numbers are defined based on the algorithm and conditions and should be used in the simulation. However, Table I contains a part that is obtained after the simulation in each step, and that is the error signal, which is calculated as (14) [14]:

$$FDM = \sum[\Delta f_1^2 + \Delta f_2^2 + \Delta p_{tie}^2]\,\Delta T \tag{14}$$

In this equation, the sum of squares equals the frequency variations of areas 1 and 2, and power changes. The parameters of DFIG and power plants are input into the simulation, and the output is observed. The resulting frequency and power output are displayed for all six conditions based on the numerical values provided in Table 1, which are substituted into Equations 7 and 8. As evident from the results, the outputs in the sixth condition are significantly more favorable than those in the first. This suggests that the system operates more efficiently under the parameters of the sixth condition, highlighting the impact of the varying factors on the overall performance. By applying the numerical values and simulating the system for a duration of 100 seconds, the simulation results are presented in Figures 6 through 17.

TABLE I.
Optimized Parameters of sssc and Smes with Fuzzy Algorithm

Optimized parameters	Case1	Case2	Case3	Case4	Case5	Case6
Ksssc	-	-	-	0.621	0.6278	0.6714
Tsssc	-	-	-	0.2563	0.212	0.2601
P1	-	-	-	0.2698	0.21	0.2989
P2	-	-	-	0.049	0.034	0.0318
P3	-	-	-	0.6	0.5037	0.5711
P4	-	-	-	0.2125	0.2254	0.2517
Ksmes	-	-	-	2.25	2.25	2
Tsmes	-	-	-	0.3015	0.2	0.2661
T1	-	-	-	0.3	0.2309	0.2972
T2	-	-	-	0.042	0.0172	0.0118
T3	-	-	-	0.7748	0.5037	0.8
T4	-	-	-	0.188	0.2088	0.1546
KI1	0.0996	0.106	0.096	-0.1486	-0.15	-0.1777
KI2	0.03	0.03	0.04	-0.068	-0.0531	-0.0603
FDM	0.05192	0.04906	0.04668	0.03515	0.3807	0.03739

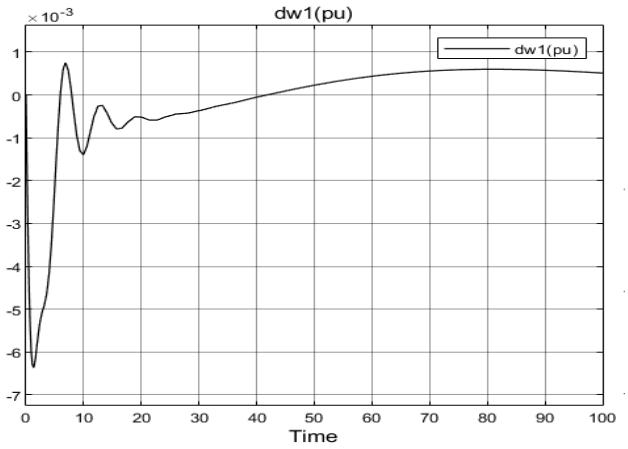

Fig. 6. Frequency output of area 1 with the sixth condition

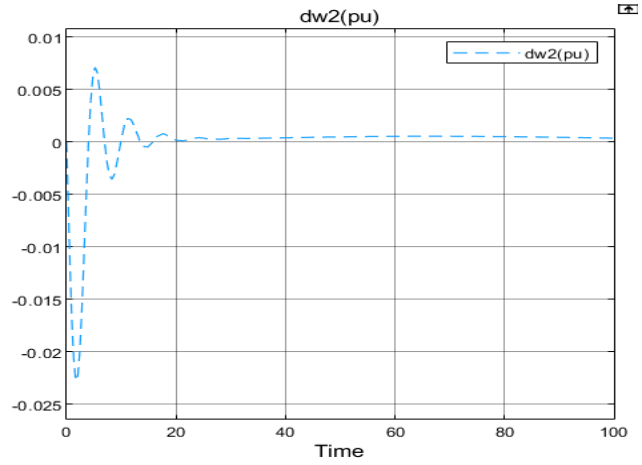

Fig. 7. Frequency output of area 2 with the sixth condition

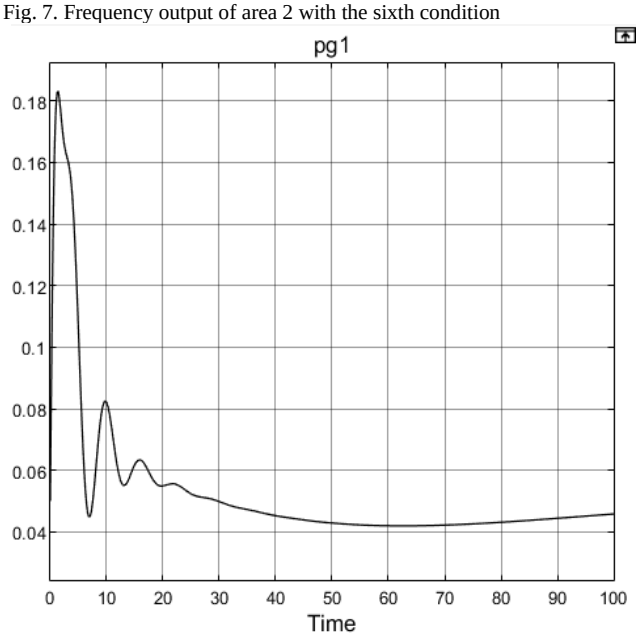

Fig. 8. Power output with the sixth condition

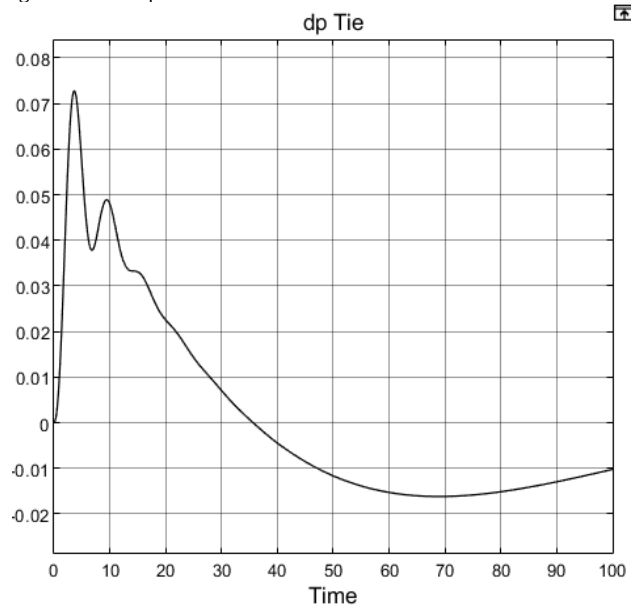

Fig. 9. Power output of the first plant with the sixth condition

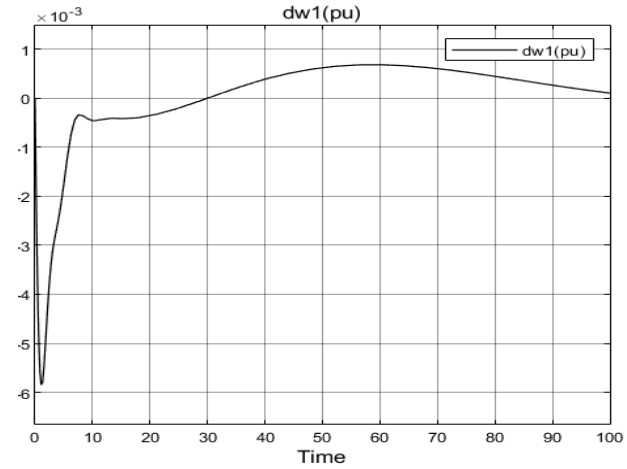

Fig. 10. Frequency output of area 1 with the fourth condition

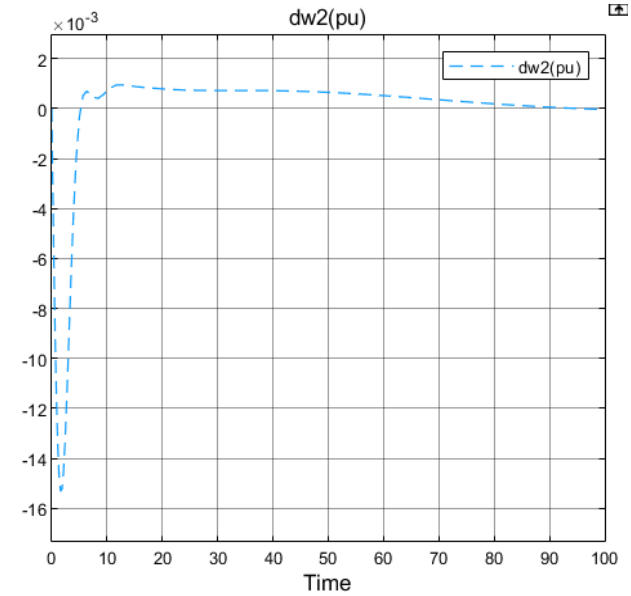

Fig. 11. Frequency output of area 2 with the fourth condition

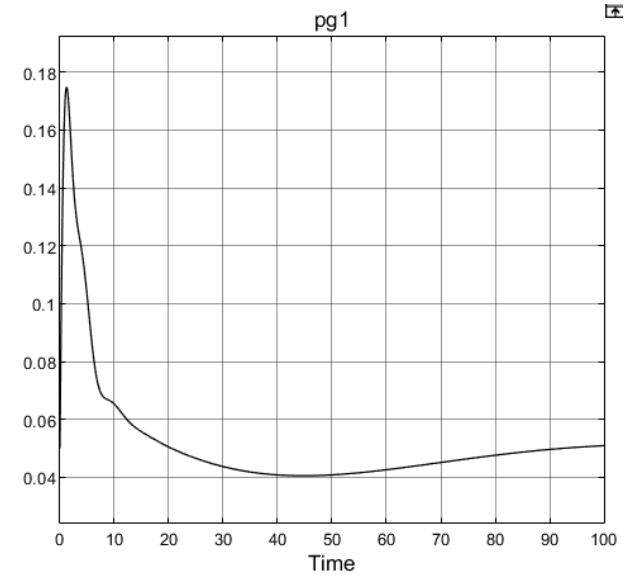

Fig. 12. Power output with the fourth condition

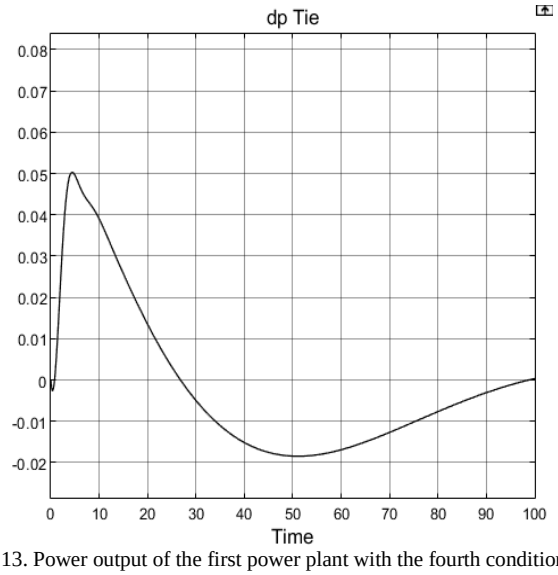

Fig. 13. Power output of the first power plant with the fourth condition

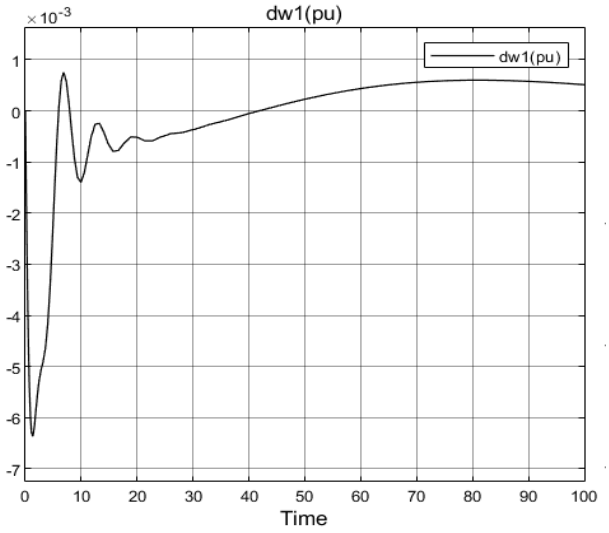

Fig. 14. Frequency output of area 1 with the first condition

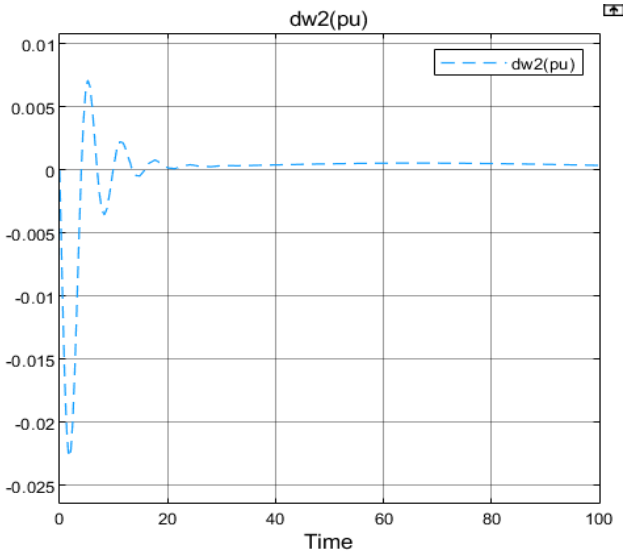

Fig. 15. Frequency output of area 2 with the first condition

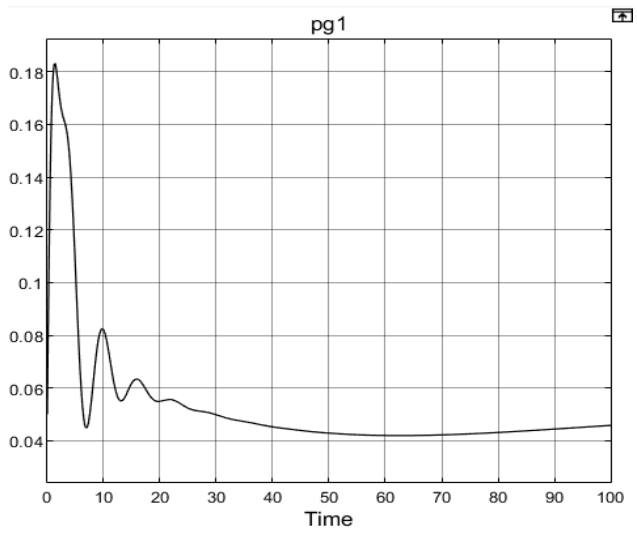

Fig. 16. Power output with the first condition

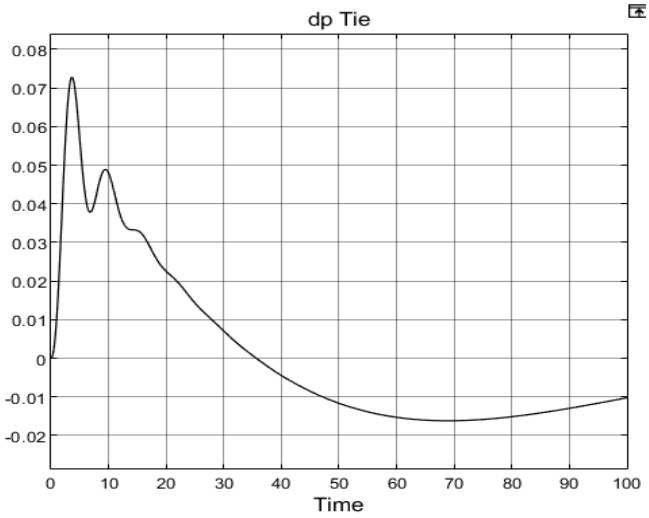

Fig. 17. Output power of the first power plant with the first condition

V. CONCLUSION

According to the previous sections, it has been found that with the sixth condition, with the presence of FACTS and SMES equipment, the amount of distortion in the output frequency is better than in the first condition, where no equipment is present in the circuit. Also, the value of the error signal decreases with the improvement of power plant inputs, but with the initial presence of equipment, a further reduction in this signal occurs. By improving the parameters of the equipment and inputs, a more optimal and appropriate value is achieved. Additionally, with the help of the fuzzy algorithm, the coefficients have improved, and the error signal has been significantly reduced. According to Table I, the value of the error signal under the first condition is 0.05192, which is reduced to its optimal value of 0.03739 under the sixth condition. Furthermore, compared with other methods, as presented in Table II, the CRPSO and RGA algorithms have been evaluated. The fuzzy algorithm demonstrates superior performance, achieving better results than these methods.

TABLE II.
Comparison of Optimized Parameters of sssc and Smes with Different Methods References

OPTIMIZED PARAMETERS	FUZZY ALGORITHM	CRPSO [20]	RGA [20]
FDM	0.03739	0.07746	0.9754

REFERENCE

[1] Dash, Puja, Arindita Saha, and Naladi Ram Babu. "Impacts of FACTS controllers in frequency regulation services of modern restructured power system." Advanced Frequency Regulation Strategies in Renewable-Dominated Power Systems. Academic Press, 2024. 307-344.

[2] Mamyrov M.N., Golovina A.V., and Belyaev A.N. Stability of LongDistance Interconnection with FACTS Controlled Devices, 2022 Conference of Russian Young Researchers in Electrical and Electronic Engineering (ElConRus), 2022, pp. 1221-1225

[3] Tripathi, S.; Singh, V.P.; Kishor, N.; Pandey, A.S. Load Frequency Control of Power System Considering Electric Vehicles' Aggregator with Communication Delay. Int. J. Electr. Power Energy Syst. 2023, 145, 108697.

[4] Naveed, A.; Sonmez, S.; Ayasun, S. Impact of Electric Vehicle Aggregator with Communication Time Delay on Stability Regions and Stability Delay Margins in Load Frequency Control System. J. Mod. Power Syst. Clean Energy 2021, 9, 595–601.

[5] Kumar, S., & Gupta, S. K. (2024, May). Enhancing the Performance of Hybrid Power System Using SMES-UPFC and Tunned with Genetic Algorithms. In 2024 International Conference on Communication, Computer Sciences and Engineering (IC3SE) (pp. 1834-1838). IEEE.

[6] Nath, V. (2024). OPTIMAL LOAD FREQUENCY CONTROL OF INTERLINKED NONLINEAR POWER SYSTEM INTEGRATED WITH SMES-TCSC AND HVDC. ASEAN Engineering Journal, 14(3), 123-136.

[7] Nagendra, K., Varun, K., Pal, G., Santosh, K., Semwal, S., Badoni, M., & Kumar, R. (2024). A Comprehensive Approach to Load Frequency Control in Hybrid Power Systems Incorporating Renewable and Conventional Sources with Electric Vehicles and Superconducting Magnetic Energy Storage. *Energies (19961073)*, *17*(23).

[8] Kumar, S., & Gupta, S. K. (2023, November). A Combined Simulink Model of Hybrid System Using SMES, TCSC Tuned Using Cuckoo Search. In *2023 9th IEEE India International Conference on Power Electronics (IICPE)* (pp. 1-6). IEEE.

[9] Kumari, S., & Pathak, P. K. (2024). A state-of-the-art review on recent load frequency control architectures of various power system configurations. *Electric Power Components and Systems*, *52*(5), 722-765.

[10] Mohamed EA, Gouda E, Mitani Y. Impact of SMES integration on the digital frequency relay operation considering high PV/wind penetration in micro-grid. Energy Procedia. 2019; 157: 1292-1304

[11] Carlini, E. M., Quaciari, C., Giannuzzi, G. M., Gadaleta, C., Pisani, C., Migliori, M., ... & Siano, G. (2024, November). Series Compensation to Increase System Stability: Static and Dynamic Assessment. In *2024 IEEE International Humanitarian Technologies Conference (IHTC)* (pp. 1-6). IEEE.

[12] Chaine S, Tripathy M. Performance of CSA optimized controllers of DFIGs and AGC to improve frequency regulation of a wind integrated hydrothermal power system. Alex Eng J. 2019; 58: 579–590.

[13] Amir, M., & Singh, K. (2024). Frequency regulation strategies in renewable energy-dominated power systems: Issues, challenges, innovations, and future trends. In *Advanced Frequency Regulation Strategies in Renewable-Dominated Power Systems* (pp. 367-381). Academic Press.

[14] PraghneshBhatt, S.P.Ghoshal, RanjitRoy,'' Coordinated control of TCPS and SMES for frequency regulation of interconnected restructured power systems with dynamic participation from DFIG based wind farm'', Elsevier Renewable Energy, Volume 40, Issue 1, Pages 40-50, April 2012.

[15] P. Kundur, Power system stability and control, McGraw-Hill, 1994.

[16]A. Modirkhazenia, O., NaghashAlmasib, Mohammad HassanKhooban,'' Improved frequency dynamic in isolated hybrid power system using an intelligent method'', Int.Journal of Electrical Power and Energy Systems, Vol 78, Pages 225-238, June 2016

[17] Kumar, V.; Sharma, V.; Naresh, R. Leader Harris Hawks Algorithm Based Optimal Controller for Automatic Generation Control in PV-Hydro-Wind Integrated Power Network. Electr. Power Syst. Res. 2023, 214, 108924.

[18] Shukla, H.; Nikolovski, S.; Raju, M.; Rana, A.S.; Kumar, P. A Particle Swarm Optimization Technique Tuned TID Controller for Frequency and Voltage Regulation with Penetration of Electric Vehicles and Distributed Generations. Energies 2022, 15, 8225.

[19] Hossam-Eldin, A.A.; Negm, E.; Ragab, M.; AboRas, K.M. A Maiden Robust FPIDD2 Regulator for Frequency-Voltage Enhancement in a Hybrid Interconnected Power System Using Gradient-Based Optimizer. Alex. Eng. J. 2022, in press.

[20] Praghnesh Bhatt, "Comparative Short Term Active Power Support from DFIG with Coordinated Control of SSSC and SMES in Restructured Power System ", Int. Journal of Electrical Power and Energy Systems, vol. 33, page. 1585-1597, 2011.